Investigations on the Active Site Models of [FeFe]-Hydrogenases: Synthesis, Structure, and Properties of N-Functionalized Azadithiolatodiiron Complexes Containing Mono- and Diphosphine Ligands

Li-Cheng Song,* Hu-Ting Wang, Jian-Hua Ge, Shu-Zhen Mei, Jie Gao, Liang-Xing Wang, Bin Gai, Li-Qun Zhao, Jing Yan, and Yong-Zhen Wang

Department of Chemistry, State Key Laboratory of Elemento-Organic Chemistry, Nankai University, Tianjin 300071, People's Republic of China

Received September 26, 2007

As the new H-cluster models, a series of N-functionalized azadithiolatodiiron complexes containing mono- and diphosphine ligands **1**–**7** have been prepared by various methods from complexes $[(\mu\text{-}SCH_2N(Fun)]Fe_2(CO)_6$ (**A**, Fun = C_6H_4CHO-*p*; **B**, Fun = $C_6H_4CO_2Me$-*p*; **C**, Fun = $CH_2CH_2O_2CCH_2C_{10}H_7$-1; **D**, Fun = CH_2CH_2OH) and $[(\mu\text{-}SCH_2)_2N(Fun)]Fe_2(CO)_5(Ph_2PH)$ (**E**, Fun = C_6H_4OMe-*p*). Treatment of **A** and **B** with 1 equiv of $Me_3NO\cdot 2H_2O$ followed by 1 equiv of Ph_3P or Ph_2PH affords the corresponding monophosphine-substituted complexes $[(\mu\text{-}SCH_2)_2N(C_6H_4CHO\text{-}p)]Fe_2(CO)_5(Ph_3P)$ (**1**) and $[(\mu\text{-}SCH_2)_2N(C_6H_4CO_2Me\text{-}p)]Fe_2(CO)_5L$ (**2**, L = Ph_3P; **3**, Ph_2PH). Further treatment of **B** with ca. 1 equiv of $Ph_2PC_2H_4PPh_2$ (dppe) produced the diphosphine dppe-bridged single model $[(\mu\text{-}SCH_2)_2N(C_6H_4CO_2Me\text{-}p)]Fe_2(CO)_4$(dppe) (**4**), whereas **C** reacts with 1 equiv of $Me_3NO\cdot 2H_2O$ followed by 0.5 equiv of $(\eta^5\text{-}Ph_2PC_5H_4)_2Fe$ (dppf) to give the diphosphine dppf-bridged double model $[(\mu\text{-}SCH_2)_2N(CH_2CH_2O_2CCH_2C_{10}H_7\text{-}1)Fe_2(CO)_5]_2$(dppf) (**5**). While **D** reacts with 1 equiv of *n*-BuLi followed by 1 equiv of Ph_2PCl or directly reacts with 1 equiv of Ph_2PCl in the presence of Et_3N to generate N-alkoxyphosphine-substituted complex $[(\mu\text{-}SCH_2)_2N(CH_2CH_2OPPh_2\text{-}\eta^1)]Fe_2(CO)_5$ (**6**), treatment of **E** with 1 equiv of *n*-BuLi followed by 1 equiv of $CpFe(CO)_2I$ yields organometallic phosphine-substituted complex $[(\mu\text{-}SCH_2)_2N(C_6H_4OMe\text{-}p)]Fe_2(CO)_5[Ph_2PFe(CO)_2Cp]$ (**7**). All the new model complexes **1**–**7** are fully characterized by elemental analysis, spectroscopy, and particularly for **1**, **3**, **4**, **6**, and **7** X-ray crystallography. More interestingly, **2** is found to be a catalyst for HOAc proton reduction to hydrogen under CV conditions. In addition, according to electrochemical and spectroelectrochemical studies, an ECEC mechanism is proposed for this electrocatalytic reaction.

Introduction

Since the high-quality crystal structures of [FeFe]-hydrogenases were elucidated,[1] a large number of structural and functional model complexes for the active site of [FeFe]-hydrogenases, the so-called H-cluster, have appeared in the literature.[2–5] Among the reported models, N-functionalized azadithiolatodiiron complexes of the type $[(\mu\text{-}SCH_2)_2N(Fun)]Fe_2(CO)_{6-n}L_n$ (Fun = functionality)[4a,b,6,7] are of particular interest. This is because (i) the azadithiolate ligand in this type of complexes is probably the actual dithiolate cofactor of [FeFe]-hydrogenases;[8] (ii) the bridgehead N atom of this ligand could play a key role in the heterolytic cleavage or formation of H_2;[9] and (iii) the bridgehead N-functionality may allow attachment of various substituents easily by functional transformation reactions.[10,11] Although numerous N-functionalized azadithiolatodiiron complexes have been so far described in the literature,[4a,b,6,7] very few studies have been carried out regarding their CO substitution and functional transformation reactions. As a continuation of our project

* To whom correspondence should be addressed. Fax: 0086-22-23504853. E-mail: lcsong@nankai.edu.cn.

(1) (a) Peters, J. W.; Lanzilotta, W. N.; Lemon, B. J.; Seefeldt, L. C *Science* **1998**, *282*, 1853. (b) Nicolet, Y.; Piras, C.; Legrand, P.; Hatchikian, E. C.; Fontecilla-Camps, J. C. *Structure* **1999**, *7*, 13.

(2) (a) Darensbourg, M. Y.; Lyon, E. J.; Smee, J. J. *Coord. Chem. Rev.* **2000**, *206–207*, 533. (b) Evans, D. J.; Pickett, C. J. *Chem. Soc. Rev.* **2003**, *32*, 268. (c) Song, L.-C. *Acc. Chem. Res.* **2005**, *38*, 21.

(3) (a) Gloaguen, F.; Lawrence, J. D.; Schmidt, M.; Wilson, S. R.; Rauchfuss, T. B. *J. Am. Chem. Soc.* **2001**, *123*, 12518. (b) Lyon, E. J.; Georgakaki, I. P.; Reibenspies, J. H.; Darensbourg, M. Y. *J. Am. Chem. Soc.* **2001**, *123*, 3268. (c) Razavet, M.; Davies, S. C.; Hughes, D. L.; Barclay, J. E.; Evans, D. J.; Fairhurst, S. A.; Liu, X.; Pickett, C. J. *Dalton Trans.* **2003**, 586. (d) Song, L.-C.; Cheng, J.; Yan, J.; Wang, H.-T.; Liu, X.-F.; Hu, Q.-M. *Organometallics* **2006**, *25*, 1544. (e) Nehring, J. L.; Heinekey, D. M. *Inorg. Chem.* **2003**, *42*, 4288.

(4) (a) Lawrence, J. D.; Li, H.; Rauchfuss, T. B. *Chem. Commun.* **2001**, 1482. (b) Song, L.-C.; Ge, J.-H.; Zhang, X.-G.; Liu, Y.; Hu, Q.-M. *Eur. J. Inorg. Chem.* **2006**, 3204. (c) Schwartz, L.; Eilers, G.; Eriksson, L.; Gogoll, A.; Lomoth, R.; Ott, S. *Chem. Comm.* **2006**, 520.

(5) (a) Song, L.-C.; Yang, Z.-Y.; Bian, H.-Z.; Hu, Q.-M. *Organometallics* **2004**, *23*, 3082. (b) Li, H; Rauchfuss, T. B *J. Am. Chem. Soc.* **2002**, *124*, 726. (c) Song, L.-C.; Yang, Z.-Y.; Hua, Y.-J.; Wang, H.-T.; Liu, Y.; Hu, Q.-M. *Organometallics* **2007**, *26*, 2106.

(6) Song, L.-C.; Ge, J.-H.; Liu, X.-F.; Zhao, L.-Q.; Hu, Q.-M. *J. Organomet. Chem.* **2006**, *691*, 5701.

(7) Stanley, J. L.; Rauchfuss, T. B.; Wilson, S. R. *Organometallics* **2007**, *26*, 1907.

(8) (a) Nicolet, Y.; Lemon, B. J.; Fontecilla-Camps, J. C.; Peters, J. W. *Trends Biochem. Sci.* **2000**, *25*, 138. (b) Nicolet, Y.; De Lacey, A. L.; Vernède, X.; Fernandez, V. M.; Hatchikian, E. C.; Fontecilla-Camps, J. C. *J. Am. Chem. Soc.* **2001**, *123*, 1596.

(9) Fan, H.; Hall, M. B. *J. Am. Chem. Soc.* **2001**, *123*, 3828.

(10) (a) Song, L.-C.; Tang, M.-Y.; Su, F.-H.; Hu, Q.-M. *Angew. Chem., Int. Ed.* **2006**, *45*, 1130. (b) Song, L.-C.; Tang, M.-Y.; Mei, S.-Z.; Huang, J.-H.; Hu, Q.-M. *Organometallics* **2007**, *26*, 1575.

(11) Tard, C.; Liu, X.; Ibrahim, S. K.; Bruschi, M.; De Gioia, L.; Davies, S. C.; Yang, X.; Wang, L.-S.; Sawers, G.; Pickett, C. J. *Nature* **2005**, *433*, 610.

10.1021/om700956e CCC: $40.75
Publication on Web 03/14/2008

Scheme 1

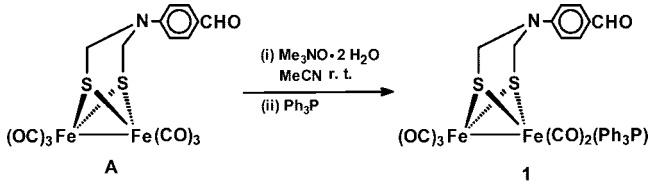

Scheme 2

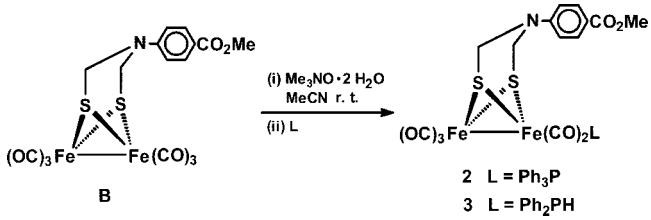

Scheme 3

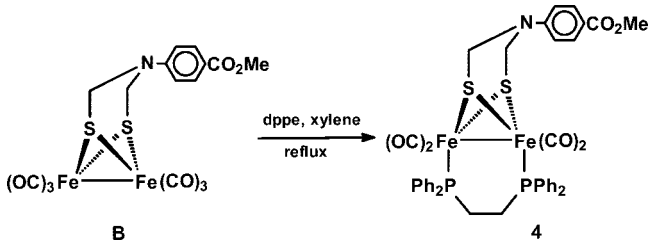

associated with N-functionalized azadithiolate (ADT) model complexes, we recently began to study their CO substitution and functional transformations aimed at obtaining N-functionalized ADT models with phosphine ligands. This is because phosphines are known to be good surrogates for cyanide ligand found in the natural enzymes.[12] In this paper, we report the synthesis, structural characterization, and electrochemical properties regarding such new complexes. Furthermore, the electrocatalytic H_2 production catalyzed by one of the synthesized new models is also described.

Results and Discussion

Synthesis and Spectroscopic Characterization of Phosphine-Containing N-Functionalized Models 1–7. Treatment of *N*-benzaldehyde complex $[(\mu\text{-}SCH_2)_2NC_6H_4CHO\text{-}p)]Fe_2(CO)_6$ (**A**)[10a] with 1 equiv of decarbonylating agent $Me_3NO\cdot 2H_2O$[3a] in MeCN at room temperature, followed by 1 equiv of Ph_3P, gave the corresponding Ph_3P-monosubstituted complex **1** in 52% yield (Scheme 1). Similarly, when *N*-benzoic ester complex $[(\mu\text{-}SCH_2)_2N(C_6H_4CO_2Me\text{-}p)]Fe_2(CO)_6$ (**B**)[6] reacted with 1 equiv of $Me_3NO\cdot 2H_2O$ followed by 1 equiv of Ph_3P or Ph_2PH, the corresponding Ph_3P- and Ph_2PH-monosubstituted complexes **2** and **3** were produced in 76% and 94% yields, respectively (Scheme 2).

Interestingly, further treatment of complex **B** with ca. 1 equiv of organic diphosphine $Ph_2PC_2H_4PPh_2$ (dppe) in refluxing xylene afforded the dppe-bridged single model **4** in 67% yield (Scheme 3), whereas naphthylacetic ester complex $[(\mu\text{-}SCH_2)_2N(CH_2\text{-}CH_2O_2CCH_2C_{10}H_7\text{-}1)]Fe_2(CO)_6$ (**C**)[13] reacted with 1 equiv of $Me_3NO\cdot 2H_2O$ followed by 0.5 equiv of organometallic diphosphine $(\eta^5\text{-}Ph_2PC_5H_4)_2Fe$ (dppf) at room temperature to give the dppf-bridged double model **5** in 30% yield (Scheme 4).

Scheme 4

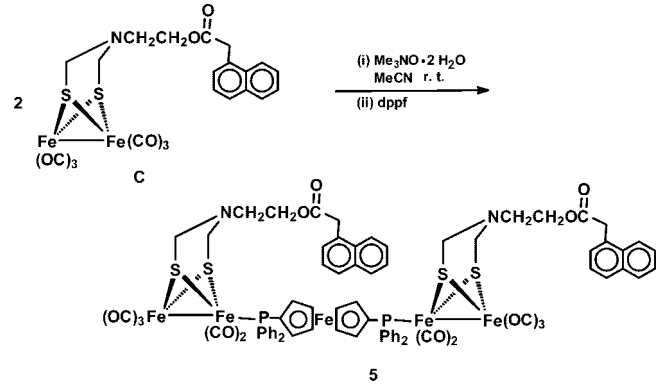

Scheme 5

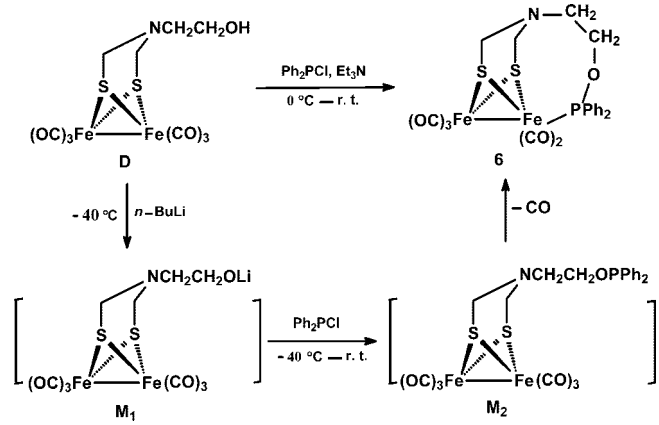

More interestingly, when *N*-hydroxyethyl complex $[(\mu\text{-}SCH_2)_2NCH_2CH_2OH]Fe_2(CO)_6$ (**D**)[13] reacted with 1 equiv of *n*-BuLi at –40 °C followed by treatment of the corresponding O−Li intermediate $\mathbf{M}_1$ with ca. 1 equiv of Ph_2PCl from –40 °C to room temperature, *N*-alkoxyphosphine-substituted complex **6** was produced in 10% yield via CO substitution of the intermediate $\mathbf{M}_2$ by its pendent alkoxyphosphine moiety (Scheme 5). Model **6** could also be prepared by a simple and convenient method with a much higher yield (53%), which involves reaction of **D** with ca. 1 equiv of Ph_2PCl in the presence of excess Et_3N from 0 °C to room temperature (Scheme 5).

In principle, the organic phosphine Ph_2PH-containing complexes such as **3** and $[(\mu\text{-}SCH_2)_2N(C_6H_4OMe\text{-}p)]Fe_2(CO)_5(Ph_2PH)$ (**E**)[4b] could be converted to organometallic phosphine-containing complexes by functionalization of their P−H bonds. For example, model **7**, which contains an extremely unstable organometallic phosphine ligand $Ph_2PFe(CO)_2Cp$,[14] might be obtained in 60% yield by reaction of **E** with 1 equiv of *n*-BuLi at –40 °C and subsequent treatment of the corresponding P−Li intermediate $\mathbf{M}_3$ with 1 equiv of $CpFe(CO)_2I$ from –40 °C to room temperature (Scheme 6).

All the new complexes **1**–**7** have been fully characterized by elemental analysis and IR, ^1H NMR, and ^{31}P NMR spectros-

(12) (a) Zhao, X.; Chiang, C.-Y.; Miller, M. L.; Rampersad, M. V.; Darensbourg, M. Y. *J. Am. Chem. Soc.* **2003**, *125*, 518. (b) Song, L.-C.; Yang, Z.-Y.; Bian, H.-Z.; Liu, Y.; Wang, H.-T.; Liu, X.-F.; Hu, Q.-M. *Organometallics* **2005**, *24*, 6126. (c) van der Vlugt, J. I.; Rauchfuss, T. B.; Wilson, S. R. *Chem.−Eur. J.* **2006**, *12*, 90. (d) Ezzaher, S.; Capon, J.-F.; Gloaguen, F.; Pétillon, F. Y.; Schollhammer, P.; Talarmin, J. *Inorg. Chem.* **2007**, *46*, 9863.

(13) Song, L.-C.; Yin, B.-S.; Li, Y.-L.; Zhao, L.-Q.; Ge, J.-H.; Yang, Z.-Y.; Hu, Q.-M. *Organometallics* **2007**, *26*, 4921.

(14) (a) Weers, J. J.; Eyman, D. P. *J. Organomet. Chem.* **1985**, *286*, 47. (b) Buckett-StLaurent, J. C. T. R.; Haines, R. J.; Nolte, C. R.; Steen, N. D. C. T. *Inorg. Chem.* **1980**, *19*, 577.

Scheme 6

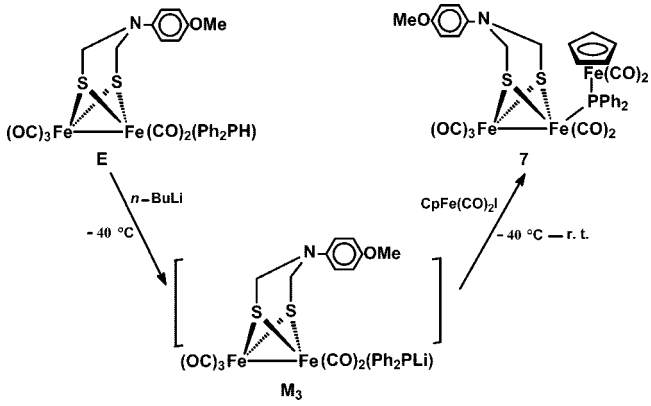

copy. The elemental analysis data of **1**–**7** are in good agreement with their compositions shown in Schemes 1, 2, 3, 4, 5, and 6. The IR spectra of **1**–**7** showed three to four absorption bands in the range 2047–1909 cm^{-1} for their terminal carbonyls, and **1**–**5** displayed one additional band in the region 1735–1695 cm^{-1} for their aldehyde and ester carbonyls. It is noteworthy that for terminal carbonyls the three IR bands of **4** are located at lower frequencies than those of **5**, which is consistent with **4** having two P donors at its diiron unit (see its crystal structure below) and **5** having only one P donor at each of its two diiron units as shown in Scheme 4.[15] In addition, the almost identical $\nu_{C\equiv O}$ IR band pattern of **5** and $[(\mu\text{-ODT})Fe_2(CO)_5]_2(dppf)$ [2047 (vs), 1983 (vs), 1933 (s)][12b] further supports that **5** has the same type of structure as that of the crystallographically characterized $[(\mu\text{-ODT})Fe_2(CO)_5]_2(dppf)$.[12b] The ^1H NMR spectra of **1**–**7** exhibited all their organic groups. For example, **1** showed a singlet at 9.79 ppm for its CHO group, **2**–**4** a singlet at ca. 3.87 ppm for their CO_2Me groups, **5** a singlet at 3.98 ppm for its CH_2 group attached to the naphthalene ring, **6** three triplets at 2.87, 3.86, and 3.91 ppm for its $N(CH_2)_2O$ group, and **7** a singlet at 4.77 ppm for its Cp group. In addition, **3** displayed a doublet at 6.24 ppm for its PH group, whereas **1**–**7** displayed two singlets or two doublets for their SCH_2N groups, respectively. The ^{31}P NMR spectrum of **3** showed a doublet at 47.20 ppm for the P atom in its Ph_2PH ligand and that of **6** a singlet at 172.47 ppm for the P atom in its *N*-alkoxyphosphine ligand, whereas the other models displayed a singlet in the range 56–65 ppm for their P atoms in the corresponding mono- and diphosphine ligands.

Crystal Structures of 1, 3, 4, 6, and 7. The molecular structures of **1**, **3**, **4**, **6**, and **7** were further investigated by X-ray crystallography. Their ORTEP plots are presented in Figures 1, 2, 3, 4, and 5, Tables 1 and 2 list the selected bond lengths and angles, respectively. As can be seen intuitively in Figures 1, 2, 3, 4, and 5, complexes **1**, **3**, **4**, **6**, and **7** all have a functionalized azadithiolate ligand bridged between two iron atoms to form two fused six-membered rings with a chair and a boat conformation, respectively. While the N-functionalized substituents of **1**, **3**, **4**, and **6** are attached to the common N1 atom of the two six-membered rings by an axial bond N1−C26, N1−C8, N1−C7, or N1−C8, the N-functionalized substituent of **7** is connected to N1 by an equatorial N1−C27 bond. Particularly noteworthy is that although the monophosphine ligands of **1**, **3**, **6**, and **7** are all located in the apical position of the square-pyramidal geometry of their iron atoms, the diphosphine ligand of **4** is connected to its two atoms with a cisoid basal/basal coordination mode. The Fe−Fe bond lengths of **1** (2.5066 Å), **3** (2.5003 Å), **4** (2.5511 Å), **6** (2.5127 Å), and **7** (2.5224 Å) are slightly shorter than the corresponding bond lengths of the phosphine-substituted complexes $[(\mu\text{-}SCH_2)_2\text{-}N(C_6H_4OMe\text{-}p)]Fe_2(CO)_5(Ph_3P)$ (2.554 Å)[4b] and $\{[(\mu\text{-}SCH_2)_2O]Fe_2(CO)_5\}_2(dppf)$ (2.5430 Å),[12b] but they are very

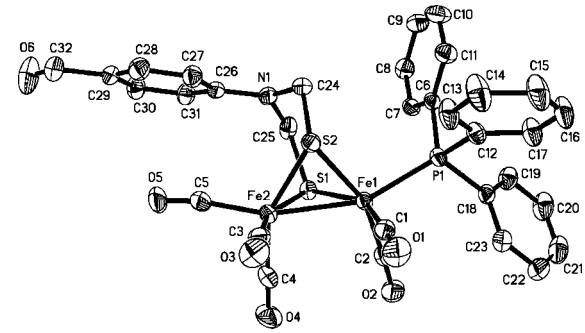

Figure 1. Molecular structure of **1** with 30% probability level ellipsoids.

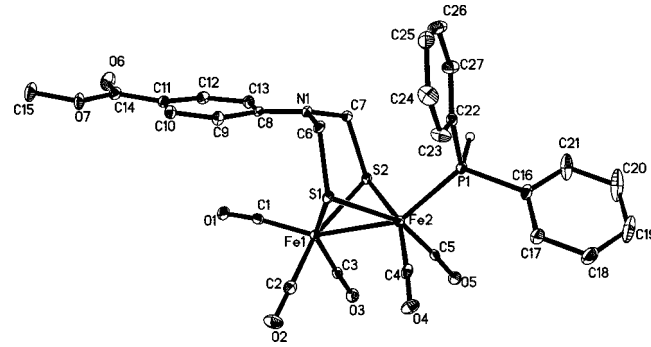

Figure 2. Molecular structure of **3** with 30% probability level ellipsoids.

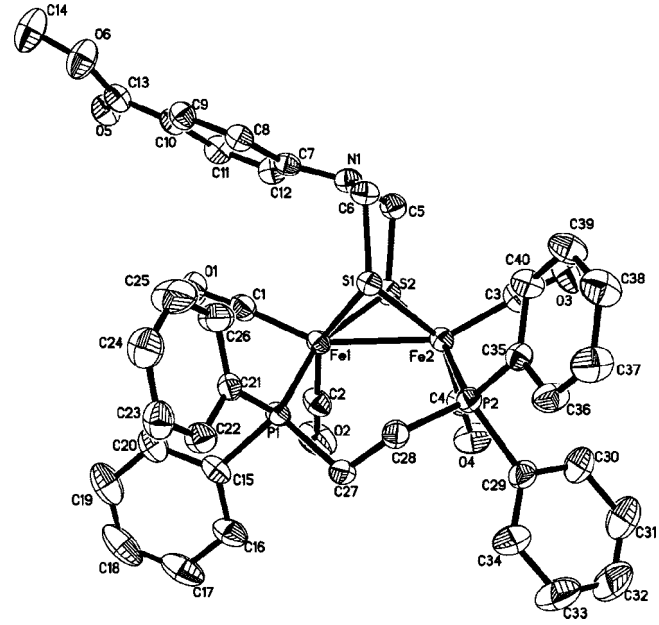

Figure 3. Molecular structure of **4** with 30% probability level ellipsoids.

(15) Collman, J. P.; Hegedus, L. S.; Norton, J. R.; Finke, R. G. *Principles and Applications of Organotransition Metal Chemistry*, 2nd ed.; University Science Books: Mill Valley, CA, 1987.

(16) Lyon, E. J.; Georgakaki, I. P.; Reibenspies, J. H.; Darensbourg, M. Y. *Angew. Chem., Int. Ed.* **1999**, *38*, 3178.

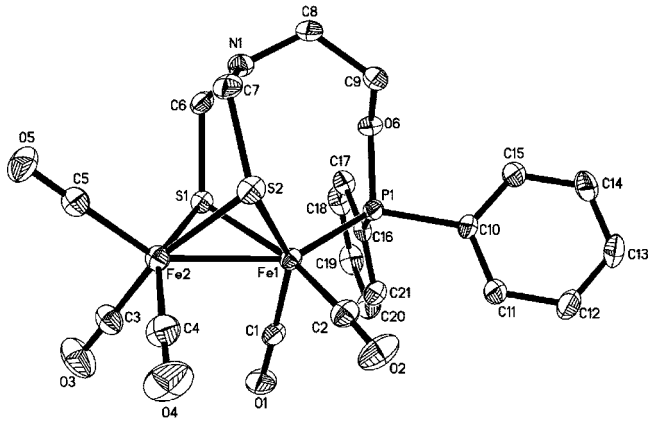

Figure 4. Molecular structure of **6** with 30% probability level ellipsoids.

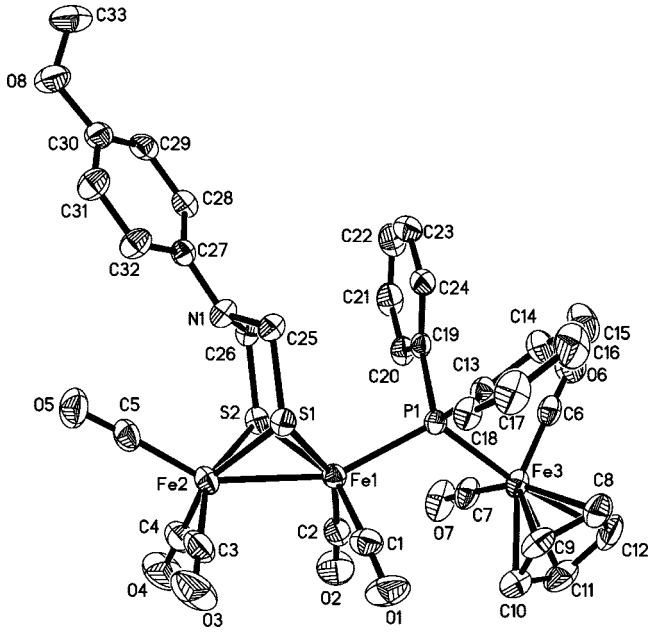

Figure 5. Molecular structure of **7** with 30% probability level ellipsoids.

close to those corresponding to the unsubstituted complexes [(μ-$SCH_2)_2N(C_6H_4OMe$-*p*)]$Fe_2(CO)_6$ (2.5076 Å),[4b] [(μ-$SCH_2)_2O$]-$Fe_2(CO)_6$ (2.5113 Å),[12b] (μ-$SCH_2)_2CH_2$]$Fe_2(CO)_6$ (2.5103 Å),[16] and [(μ-$SCH_2)_2$NMe]$Fe_2(CO)_6$ (2.4924 Å).[17] It is interesting to note that the [2Fe2SP] model complex **6** and the [3Fe2SP] model complex **7** are structurally very similar to the previously reported [2Fe3S] and [3Fe3S] model complexes, respectively.[4a,12b,18]

Electrochemistry, Electrocatalysis, and Spectroelectrochemistry (SEC) of 2. In order to examine the electrocatalytic H_2-producing ability of the phosphine-containing H-cluster models,[19,20] we initiated a study on electrochemical properties of **2** by using cyclic voltammetry (CV). As can be seen in Figure 6, in the absence of HOAc, **2** displays one quasi-reversible reduction event at −1.67 V (its second reduction is beyond the electrochemical window of solvent MeCN) and two irreversible oxidation events at +0.34 and +0.61 V. The three observed redox events are all one-electron processes, which were supported by the calculated value of 0.94 faraday/equiv (obtained through study of bulk electrolysis of a MeCN solution of **2** at −1.87 V) and the calculated value of $(i_p/\nu^{1/2})/(it^{1/2}) = 3.6$ (obtained through study of CV and chronoamperometry (CA) of **2**).[21] In addition, they could be assigned to the reduction of Fe^IFe^I to Fe^IFe^0, the oxidation of Fe^IFe^I to Fe^IFe^{II}, and the oxidation of Fe^IFe^{II} to $Fe^{II}Fe^{II}$, respectively. The electrochemical behavior of **2** is very similar to that of its parent complex **B**, except that the observed reduction and oxidation peaks of **2** are shifted toward the cathodic direction by an average 200 mV, as compared to those corresponding to complex **B**.[6] Actually, such cathodic shifts are due to the increase of electron density at its diiron center originated from replacement of a CO ligand of **B** by the stronger electron-donating ligand Ph_3P.

The cyclic voltammogram of **2** in the presence of HOAc is shown in Figure 7. For comparison, the cyclic voltammogram of **2** without HOAc is also included. As shown in Figure 7, when 1–9 mM HOAc was added, the initial first reduction peak of **2** at −1.67 V slightly increased, but it did not grow with sequential addition of the acid. In addition, upon addition of 1–9 mM HOAc, a new reduction peak at ca. −2.13 V appeared, which grew dramatically with increasing concentration of the acid. These observations are typical of a catalytic proton reduction process.[6,20,22] To further confirm this, we carried out bulk electrolysis of a MeCN solution containing HOAc (25 mM) and **2** (0.5 mM) at −2.20 V. During 0.5 h of the bulk electrolysis, 14.6 F per mol of **2** passed, which corresponds to 7.3 turnovers. Gas chromatography showed that the hydrogen yield is >90%.

According to the above-mentioned electrochemical observations and the reported similar cases,[6,20,22] we might proposed an ECEC (E = electrochemical, C = chemical) mechanism for this electrocatalytic H_2-producing process as shown in Scheme 7. First, **2** is reduced at −1.67 V to give monoanion $\mathbf{2}^-$. Then, $\mathbf{2}^-$ is protonated by HOAc to generate the neutral Fe−H species **2H**. After **2H** is further reduced at –2.13 V, the resulting anionic Fe−H species can be protonated by HOAc to reproduce **2** with evolution of H_2 to complete the catalytic cycle. It follows that this ECEC mechanism is different from the EECC mechanism suggested for reduction of a HOAc proton to H_2 catalyzed by complex **B**.[6] It is evident that the major reason causing such a difference is that one CO ligand of **B** had been replaced by stronger electron-donating Ph_3P. In fact, while Ph_3P makes the first reduction of **2** more difficult than that of **B** ($E_{pc} = -1.67$ versus −1.54 V), it can make the one-electron-reduced monoanion $\mathbf{2}^-$ more electron-rich than the corresponding $\mathbf{B}^-$ and thus be directly protonated by weak acid HOAc to cause the ECEC mechanism.

In order to gain more evidence to support the electrocatalytic mechanism shown in Scheme 7, we further carried out the spectroelectrochemical study of **2** by using IR SEC techniques[22,23] (Figures 8 and 9). In Figure 8, for comparison the IR spectrum of **2** without HOAc recorded prior to the application of the potential (Figure 8a) is included. As the electrolysis proceeded, the three ν(CO) IR bands at 2049, 1990, and 1930 cm^{-1} of the

(17) Lawrence, J. D.; Li, H.; Rauchfuss, T. B.; Bénard, M.; Rohmer, M.-M. *Angew. Chem., Int. Ed.* **2001**, *40*, 1768.
(18) Razavet, M.; Davies, S. C.; Hughes, D. L.; Pickett, C. J. *Chem. Commun.* **2001**, 847.
(19) Mejia-Rodriguez, R.; Chong, D.; Reibenspies, J. H.; Soriaga, M. P.; Darensbourg, M. Y. *J. Am. Chem. Soc.* **2004**, *126*, 12004.
(20) Gloaguen, F.; Lawrence, J. D.; Rauchfuss, T. B. *J. Am. Chem. Soc.* **2001**, *123*, 9476.
(21) Zanello, P. *Inorganic Electrochemistry. Theory, Practice and Application*; Thomas Graham House: Cambridge, UK, 2003.
(22) Chong, D.; Georgakaki, I. P.; Mejia-Rodriguez, R.; Sanabria-Chinchilla, J.; Soriaga, M. P.; Darensbourg, M. Y. *Dalton Trans.* **2003**, 4158.
(23) Borg, S. J.; Behrsing, T.; Best, S. P.; Razavet, M.; Liu, X.; Pickett, C. J. *J. Am. Chem. Soc.* **2004**, *126*, 16988.

Table 1. Selected Bond Lengths (Å) and Angles (deg) for 1, 3, and 4

		1	
Fe(1)−S(1)	2.2904(13)	Fe(2)−S(2)	2.2866(13)
Fe(1)−S(2)	2.2784(14)	N(1)−C(24)	1.427(6)
Fe(1)−Fe(2)	2.5066(9)	N(1)−C(26)	1.401(5)
Fe(2)−S(1)	2.2640(13)	Fe(1)−P(1)	2.2562(13)
S(1)−Fe(1)−S(2)	83.72(4)	S(2)−Fe(2)−Fe(1)	56.54(4)
S(1)−Fe(1)−Fe(2)	56.11(4)	Fe(2)−S(1)−Fe(1)	66.78(4)
S(2)−Fe(1)−Fe(2)	56.85(4)	C(24)−N(1)−C(26)	120.6(4)
S(1)−Fe(2)−S(2)Fe(1)−S(1)	84.12(5)	P(1)−Fe(1)−S(2)Fe(2)−S(2)2.2822(8)	104.27(5)
		3	
Fe(1)−S(2)	202822(8)	Fe(2)−S(2)	2.2755(9)
Fe(1)−S(2)	2.2764(9)	N(1)−C(6)	1.433(3)
Fe(1)−Fe(2)	2.5003(9)	N(1)−C(8)	1.402(2)
Fe(2)−S(1)	2.2711(9)	Fe(2)−P(1)	2.2231(8)
S(2)−Fe(1)−S(1)	84.29(2)	S(1)−Fe(2)−Fe(1)	56.906(19)
S(1)−Fe(1)−Fe(2)	56.48(3)	P(1)−Fe(2)−S(1)	107.81(3)
S(2)−Fe(2)−Fe(1)	56.70(3)	S(1)−Fe(2)−S(2)	84.56(3)
Fe(2)−S(1)−Fe(1)Fe(2)−S(2)−Fe(1)Fe(1)−S(1)	66.61(3)	C(6)−N(1)−C(7)	112.29(18)
Fe(2)−S(1)−Fe(1)Fe(2)−S(2)−Fe(1)Fe(1)−S(1)	66.64(3)	o(7)-C(14)−C(11)	111.29(18)
		4	
Fe(1)−S(1)	2.2463(6)	Fe(2)−S(2)	2.2615(7)
Fe(1)−S(2)	2.2820(6)	Fe(1)−P(1)	2.2166(7)
Fe(1)−Fe(2)	2.5511(5)	P(1)−C(27)	1.838(2)
Fe(2)−S(1)	2.2682(6)	N(1)−C(5)	1.435(3)
P(1)−Fe(1)−S(1)	90.67(2)	S(1)−Fe(1)−Fe(2)	55.998(18)
S(1)−Fe(2)−S(2)	84.46(2)	S(1)−Fe(2)−Fe(1)	55.188(16)
P(1)−Fe(1)−Fe(2)	106.34(2)	Fe(1)−S(1)−Fe(2)	68.814(18)
P(2)−Fe(2)−S(2)	163.22(2)	C(15)−P(1)−Fe(1)C(5)−N(1)−C(6)	114.10(8)
S(2)−Fe(2)−S(1)	84.44(2)	C(5)−N(1)−C(6)	112.92(18)

Table 2. Selected Bond Lengths (Å) and Angles (deg) for 6 and 7

		6	
Fe(1)−S(1)	2.2556(10)	Fe(2)−S(2)	2.2690(11)
Fe(1)−S(2)	2.2821(10)	N(1)−C(8)	1.444(4)
Fe(1)−Fe(2)	2.5127(7)	P(1)−O(6)	1.614(2)
Fe(2)−S(1)	2.2776(10)	Fe(1)−P(1)	2.2056(10)
S(2)−Fe(1)−S(1)	84.18(3)	S(2)−Fe(1)−Fe(2)	56.24(3)
S(1)−Fe(2)−Fe(1)	55.92(3)	S(1)−Fe(1)−Fe(2)	56.76(3)
S(2)−Fe(2)−Fe(1)	56.74(3)	S(2)−Fe(2)−S(1)	83.97(4)
Fe(2)−S(1)−Fe(1)	67.32(3)	C(6)−N(1)−C(7)	116.9(3)
Fe(2)−S(1)−Fe(1)	67.02(3)	O(6)−P(1)−Fe(1)	115.28(9)
		7	
Fe(1)−S(1)	2.2607(10)	Fe(2)−S(2)	2.2706(10)
Fe(1)−S(2)	2.2662(10)	Fe(1)−P(1)	2.2905(10)
Fe(1)−Fe(2)	2.5224(7)	Fe(3)−P(1)	2.3355(10)
Fe(2)−S(1)	2.2626(10)	N(1)−C(25)	1.442(4)
S(2)−Fe(1)−S(1)	84.29(3)	S(2)−Fe(2)−Fe(1)	56.14(3)
S(2)−Fe(1)−Fe(2)	56.30(3)	Fe(2)−S(1)−Fe(1)	67.79(3)
S(1)−Fe(1)−Fe(2)	56.14(3)	Fe(1)−S(2)−Fe(2)	67.56(3)
S(1)−Fe(2)−S(2)	84.15(3)	Fe(1)−P(1)−Fe(3)	116.70(4)
S(1)−Fe(2)−Fe(1)	56.07(3)	C(26)−N(1)−C(25)	114.6(2)

initial **2** decreased in their intensities with the growth of new bands at lower frequencies. When the electrolysis was completed (ca. 1.1 equiv electron passed), the IR spectrum showed three new ν(CO) bands at 2013, 1972, and 1906 cm^{-1} (Figure 8b). These bands were shifted toward lower frequencies relative to the original ones by an average of 26 cm^{-1} and could be reasonably attributed to the formation of monoanion $\mathbf{2}^-$.[15] The EPR spectrum of the catholyte of **2** was recorded at 120 K, which displayed a strong signal with $g_\perp = 2.064$ and a weak signal with $g_\parallel = 1.994$, indicating the odd-electron species (Fe^IFe^0) generated by bulk electrolysis of **2**.[22] The IR spectrum of **2** with HOAc recorded prior to the electrolysis (Figure 9a) is essentially the same as that of **2** without HOAc (Figure 8a). This means that **2** cannot be directly protonated by the weak acid HOAc. As can be seen in Figure 9b, when the electrolysis of **2** with HOAc was finished (ca. 1.1 equiv electron passed), five new ν(CO) bands at 2076, 2036, 1996, 1976, and 1932 cm^{-1} appeared in higher frequencies. Such IR shifts toward higher frequencies might be reasonably ascribed to the formation of the Fe(II)−H species **2H** from protonation of monoanion $\mathbf{2}^-$ by HOAc.[15] It follows that the studied results of electrochemistry, IR, and EPR spectroelectrochemistry have provided evidence to support the ECEC mechanism, although more evidence is still needed for the detailed mechanism.

Conclusion

The N-functionalized diiron azadithiolate phosphine complexes **1**–**7** as the new H-cluster models have been prepared from the corresponding complexes **A**−**E** via four different synthetic methods: (i) Me_3NO-promoted CO substitution; (ii) thermally induced CO substitution; (iii) N-functional transformation followed by CO substitution; and (iv) functional transformation of ligand Ph_2PH in its coordination sphere. Particularly interesting are methods iii and iv, since they can provide simple and convenient routes leading to novel model complexes **6** and **7**, which structurally resemble the [2Fe3S]

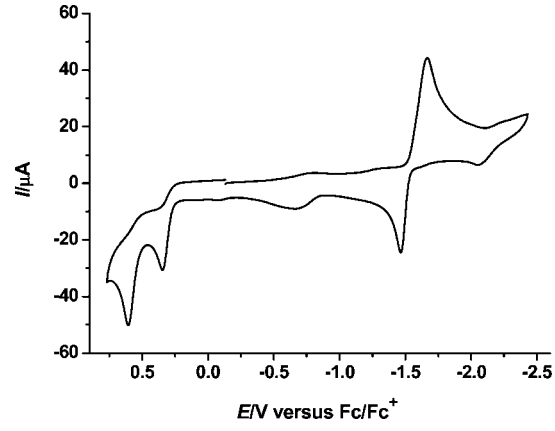

Figure 6. Cyclic voltammogram of **2** (1.0 mM) without HOAc in 0.1 M n-Bu_4NPF_6/MeCN at a scan rate of 100 mV s^{-1}.

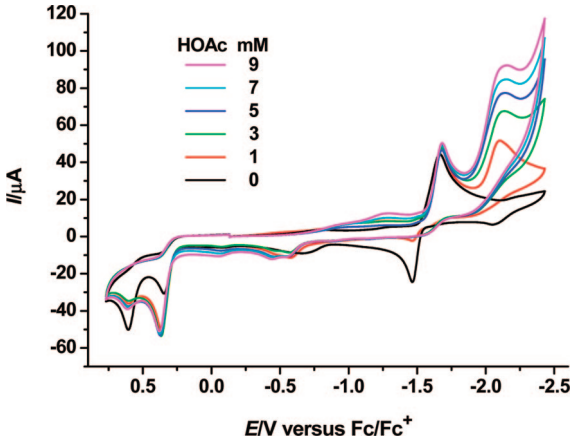

Figure 7. Cyclic voltammograms of **2** (1.0 mM) with and without HOAc (0–9 mM) in 0.1 M n-Bu_4NPF_6/MeCN at a scan rate of 100 mV s^{-1}.

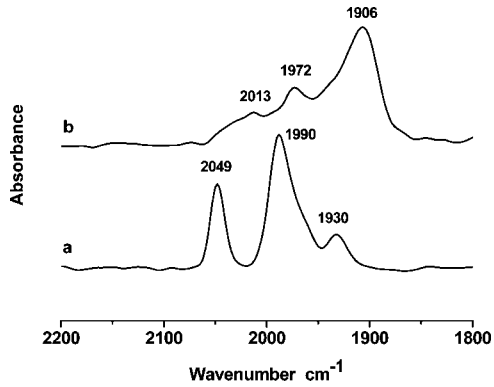

Figure 8. IR spectra in the CO region recorded during the electrolysis of 5 mM **2** without HOAc in CO-saturated MeCN (0.1 M n-Bu_4NPF_6) at −1.82 V: (a) prior to the application of the potential; (b) electrolysis for 2 h.

Scheme 7

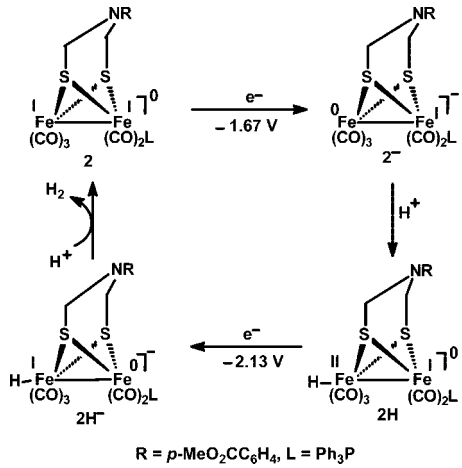

models reported by the Rauchfuss and Pickett groups,[4a,18] as well as the [3Fe3S] model previously reported by us, respectively.[12b] All the new models **1–7** have been fully characterized, whereas model **2**, the Ph_3P-monosubstituted derivative of **B**, has been found to be a catalyst for H_2 production under electrochemical conditions. Both electrochemical and spectroelectrochemical data of **2** strongly support the suggested ECEC mechanism for the electrochemical H_2 production catalyzed by **2**. Further studies concerning the synthetic methodology and biomimetically catalytic function of such H-cluster models are in progress.

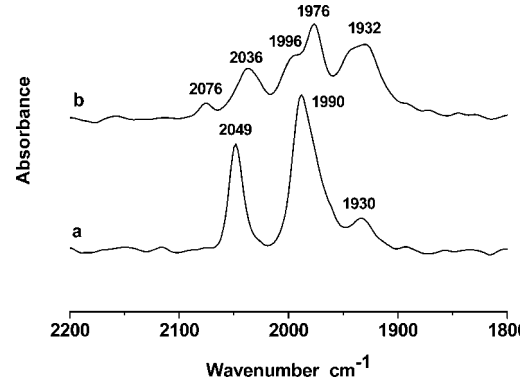

Figure 9. IR spectra in the CO region recorded during the electrolysis of 5 mM **2** with 50 mM HOAc in CO-saturated MeCN solution (0.1 M n-Bu_4NPF_6) at −1.82 V: (a) prior to the application of the potential; (b) electrolysis for 2 h.

Experimental Section

General Comments. All reactions were performed using standard Schlenk and vacuum-line techniques under N_2. Acetonitrile was distilled once from P_2O_5 and then from CaH_2 under N_2. THF and xylene were purified by distillation under N_2 from sodium/benzophenone ketyl. While [(μ-SCH_2)$_2$$NC_6H_4CHO$-$p$)]$Fe_2(CO)_6$ (**A**),[10a] [(μ-SCH_2)$_2$$N(C_6H_4CO_2Me$-$p$)]$Fe_2(CO)_6$ (**B**),[6] [(μ-SCH_2)$_2$N-($CH_2CH_2O_2CCH_2C_{10}H_7$-1)]$Fe_2(CO)_6$ (**C**),[13] [(μ-SCH_2)$_2$$NCH_2CH_2$-OH]$Fe_2(CO)_6$ (**D**),[13] [(μ-SCH_2)$_2$$N(C_6H_4OMe$-$p$)]$Fe_2(CO)_5(Ph_2PH)$ (**E**),[4b] Ph_2PH,[24] (η^5-$Ph_2PC_5H_4$)$_2$Fe (dppf),[25] and $CpFe(CO)_2I$[26] were prepared according to literature procedures, the other starting materials were commercially available and used without further purification. Preparative TLC was carried out on glass plates (26 × 20 × 0.25 cm) coated with silica gel H (10−40 μm). IR spectra were recorded on a Bio-Rad FTS 6000 spectrophotometer. ^{1}H NMR and ^{31}P NMR spectra were obtained on a Bruker Avance 300 or a Varian Mercury Plus 400 spectrometer. A Bruker EMX EPR spectrometer was used to collect electron paramagnetic resonance spectra. Elemental analyses were performed on an Elementar Vario EL analyzer. Melting points were determined on a Yanaco MP-500 apparatus and were uncorrected.

Preparation of [(μ-SCH_2)$_2$$N(C_6H_4CHO$-$p$)]$Fe_2(CO)_5(Ph_3P)$ (1). To a red solution of **A** (0.140 g, 0.28 mmol) in MeCN (10 mL) was added $Me_3NO\cdot 2H_2O$ (0.032 g, 0.28 mmol). The mixture was stirred at room temperature for 20 min to give a brown-black solution. After Ph_3P (0.074 g, 0.28 mmol) was added, the new mixture was stirred at this temperature for 4 h. Volatiles were removed under vacuum, and the residue was subjected to TLC using acetone/petroleum ether (v/v = 1:3) as eluent. From the main red band, **1** was obtained as a dark red solid (0.106 g, 52%), mp 206–207 °C. Anal. Calcd for $C_{32}H_{24}Fe_2NO_6PS_2$: C, 52.99; H, 3.34; N, 1.93. Found: C, 52.73; H, 3.30; N, 2.13. IR (KBr disk): $\nu_{C\equiv O}$ 2047 (vs), 1985 (vs), 1926 (s); ν_{CHO} 1695 (m) cm^{-1}. ^{1}H NMR (300 MHz, $CDCl_3$): 2.89 (br s, 2H, 2C*H*HS), 4.12 (br s, 2H, 2CH*H*S), 6.63–7.73 (m, 19H, C_6H_4, $3C_6H_5$), 9.79 (s, 1H, CHO) ppm. ^{31}P NMR (121 MHz, $CDCl_3$, 85% H_3PO_4): 64.30 (s) ppm.

Preparation of [(μ-SCH_2)$_2$$N(C_6H_4CO_2Me$-$p$)]$Fe_2(CO)_5(Ph_3P)$ (2). To a red solution of **B** (0.130 g, 0.25 mmol) in MeCN (20 mL) was added $Me_3NO\cdot 2H_2O$ (0.029 g, 0.25 mmol). The mixture was

(24) Kuchen, W.; Buchwald, H. *Chem. Ber.* **1958**, *91*, 2871.
(25) Bishop, J. J.; Davison, A.; Katcher, M. L.; Lichtenberg, D. W.; Merrill, R. E.; Smart, J. C. *J. Organomet. Chem.* **1971**, *27*, 241.
(26) King, R. B. *Organometallic Syntheses, Transition-Metal Compounds*; Academic Press: New York, 1965; Vol. I, p 175.

Table 3. Crystal Data and Structure Refinement Details for 1, 3, and 4

	1	3	4
mol formula	$C_{32}H_{24}Fe_2NO_6PS_2$ CH_2Cl_2	$_{27}H_{22}Fe_2NO_7PS_2$	$C_{40}H_{35}Fe_2NO_6P_2S_2$
mol wt	810.24	679.25	863.45
cryst syst	monoclinic	triclinic	monoclinic
space group	$P2(1)/c$	$P\bar{1}$	$P2(1)/n$
a /Å	12.753(3)	9.679(3)	9.3759(13)
b /Å	17.823(4)	12.785(5)	19.560(3)
c /Å	15.462(4)	12.908(4)	21.756(3)
α /deg	90	71.734(11)	90
β /deg	90.205(4)	68.835(13)	94.719(2)
γ /deg	90	77.581(13)	90
V/Å^3	3514.4(14)	1405.1(8)	3976.4(10)
Z	4	2	4
D_c/g cm^{-3}	1.531	1.605	1.442
abs coeff/mm^{-1}	1.186	1.285	0.962
F(000)	1648	692	1776
index ranges	$-14 \le h \le 16$ $-22 \le k \le 19$ $-19 \le l \le 18$	$-12 \le h \le 12$ $-16 \le k \le 16$ $-16 \le l \le 16$	$-12 \le h \le 12$ $-25 \le k \le 25$ $-28 \le l \le 28$
no. of rflns	19 802	16 487	48 732
no. of indep rflns	7187	6667	9465
$2\theta_{max}$/deg	51.04	55.74	55.74
R	0.0480	0.0354	0.0404
R_w	0.1014	0.0744	0.0990
goodness of fit	1.005	1.043	1.091
largest diff peak and hole/e Å^{-3}	0.687/−0.509	0.473/−0.349	0.404/−0.361

Table 4. Crystal Data and Structure Refinement Details for 6 and 7

	6	7
mol formula	$C_{21}H_{18}Fe_2NO_6PS_2$	$C_{33}H_{26}Fe_3NO_8PS_2$
mol wt	587.15	827.19
cryst syst	monoclinic	triclinic
space group	$P2(1)/n$	$P\bar{1}$
a/Å	12.519(2)	11.090(2)
b/Å	17.022(3)	12.673(3)
c/Å	12.706(2)	14.953(3)
α/deg	90	89.762(4)
β/deg	119.186(3)	69.865(3)
γ/deg	90	64.380(3)
V/Å^3	2363.8(7)	1752.9(6)
Z	4	2
D_c/g cm^{-3}	1.650	1.567
abs coeff/mm^{-1}	1.510	1.440
F(000)	1192	840
index ranges	$-15 \le h \le 15$ $-21 \le k \le 21$ $-8 \le l \le 15$	$-13 \le h \le 13$ $-15 \le k \le 10$ $-18 \le l \le 15$
no. of rflns	13 169	9981
no. of indep rflns	4799	7071
$2\theta_{max}$/deg	52.66	52.80
R	0.0404	0.0380
R_w	0.0750	0.0842
goodness of fit	1.054	1.013
largest diff peak and hole/e Å^{-3}	0.636/−0.328	0.409/−0.374

stirred at room temperature for 20 min, and then Ph_3P (0.065 g, 0.25 mmol) was added. After the new mixture was stirred at this temperature for 3 h, volatiles were removed under vacuum and the residue was subjected to TLC using CH_2Cl_2/petroleum ether (v/v = 1:2) as eluent. From the main red band, **2** was obtained as a dark red solid (0.144 g, 76%), mp 172 °C (dec). Anal. Calcd for $C_{33}H_{26}Fe_2NO_7PS_2$: C, 52.47; H, 3.47; N, 1.85. Found: C, 52.05; H, 3.75; N, 2.01. IR (KBr disk): $\nu_{C\equiv O}$ 2046 (vs), 1987 (vs), 1933 (s); $\nu_{C=O}$ 1713 (s) cm^{-1}. ^{1}H NMR (300 MHz, $CDCl_3$): 2.95 (d, J = 12.9 Hz, 2H, 2C *H*HS), 3.86 (s, 3H, OCH_3), 4.13 (d, J = 12.9 Hz, 2H, 2CH *H*S), 6.56, 6.59, 7.87,7.90 (AB quartet, 4H, C_6H_4), 7.47–7.76 (m, 15H, $3C_6H_5$) ppm. ^{31}P NMR (121 MHz, $CDCl_3$, 85% H_3PO_4): 64.41 (s) ppm.

Preparation of [(μ-SCH$_2$)$_2$N(C$_6$H$_4$CO$_2$Me-*p*)]Fe$_2$(CO)$_5$(Ph$_2$PH) (3). Similarly, from complex **B** (0.130 g, 0.25 mmol), $Me_3NO \cdot 2H_2O$ (0.029 g, 0.25 mmol), Ph_2PH (0.047 g, 0.25 mmol), and MeCN (20 mL), **3** was obtained as a red solid (0.159 g, 94%), mp 144–145 °C. Anal. Calcd for $C_{27}H_{22}Fe_2NO_7PS_2$: C, 47.74; H, 3.26; N, 2.06. Found: C, 47.99; H, 3.27; N, 1.98. IR (KBr disk): $\nu_{C\equiv O}$ 2041 (vs), 1957 (vs), 1926 (vs); $\nu_{C=O}$ 1704 (s) cm^{-1}. ^{1}H NMR (300 MHz, $CDCl_3$): 3.88 (s, 3H, OCH_3), 4.14 (d, J = 13.2 Hz, 2H, 2C*H*HS), 4.23 (d, J = 13.2 Hz, 2H, 2CH*H*S), 6.24 (d, J_{PH} = 350 Hz, 1H, PH), 6.62, 6.65, 7.90, 7.93 (AB quartet, 4H, C_6H_4), 7.42–7.68 (m, 10H, $2C_6H_5$) ppm. ^{31}P NMR (121 MHz, $CDCl_3$, 85% H_3PO_4): 47.20 (d, J_{PH} = 350 Hz) ppm.

Preparation of [(μ-SCH$_2$)$_2$N(C$_6$H$_4$CO$_2$Me-*p*)]Fe$_2$(CO)$_4$(dppe) (4). A red solution of **B** (0.092 g, 0.18 mmol) and $Ph_2PC_2H_4PPh_2$ (dppe, 0.080 g, 0.20 mmol) in xylene (20 mL) was refluxed for 2 h. The same workup as that for the preparation of **2** using CH_2Cl_2/petroleum ether (v/v = 4:1) as eluent gave **4** as a red solid (0.102 g, 67%), mp 122–123 °C. Anal. Calcd for $C_{40}H_{35}Fe_2NO_6P_2S_2$: C, 55.64; H, 4.09; N, 1.62. Found: C, 55.85; H, 4.35; N, 1.59. IR (KBr disk): $\nu_{C\equiv O}$ 1990 (s), 1955 (vs), 1923 (s); $\nu_{C=O}$ 1706 (m) cm^{-1}. ^{1}H NMR (400 MHz, $CDCl_3$): 2.30 (br s, 2H, $2PCH_2$), 3.86 (s, 3H, OCH_3), 4.33 (s, 2H, 2C*H*HS), 4.51 (s, 2H, 2CH*H*S), 7.39–7.81 (m, 20H, $4C_6H_5$), 6.77, 6.80, 7.98, 8.01 (AB quartet, 4H C_6H_4) ppm. ^{31}P NMR (121 MHz, $CDCl_3$, 85% H_3PO_4): 60.80 (s) ppm.

Preparation of [(μ-SCH$_2$)$_2$N(CH$_2$CH$_2$O$_2$CCH$_2$C$_{10}$H$_7$-1)Fe$_2$(CO)$_5$]$_2$(dppf) (5). To a red solution of **C** (0.142 g, 0.24 mmol) in MeCN (10 mL) was added $Me_3NO \cdot 2H_2O$ (0.026 g, 0.24 mmol), and then the mixture was stirred at room temperature for 20 min. After dppf (0.066 g, 0.12 mmol) was added, the new mixture was stirred at room temperature for 4 h. The same workup as that for the preparation of **2** using acetone/petroleum ether (v/v = 1:4) as eluent produced **5** as a red solid (0.060 g, 30%), mp 78–80 °C. Anal. Calcd for $C_{76}H_{62}Fe_5N_2O_{14}P_2S_4$: C, 53.80; H, 3.68; N, 1.65. Found: C, 54.06; H, 3.89; N, 1.84. IR (KBr disk): $\nu_{C\equiv O}$ 2042 (vs), 1980 (vs), 1926 (s); $\nu_{C=O}$ 1735 (s), cm^{-1}. ^{1}H NMR (400 MHz, $CDCl_3$): 2.24–2.28 (m, 8H, 4C*H*HS, $2NCH_2CH_2O$), 2.59 (d, 4H, J = 11.2 Hz, 4CH*H*S), 3.65 (s, 4H, $2NCH_2CH_2O$), 3.98 (s, 4H, $2CH_2C_{10}H_7$), 4.16–4.25 (m, 8H, $2C_5H_4$), 7.26–7.89 (m, 34H, $4C_6H_5$, $2C_{10}H_7$) ppm. ^{31}P NMR (162 MHz, $CDCl_3$, 85% H_3PO_4): 56.46 (s) ppm.

Preparation of [(μ-SCH$_2$)$_2$N(CH$_2$CH$_2$OPPh$_2$-η^1)]Fe$_2$(CO)$_5$ (6). Method i: A red solution of **D** (0.100 g, 0.23 mmol) in THF (5 mL) was cooled to –40 °C, and then *n*-BuLi (1 M in hexane, 0.23

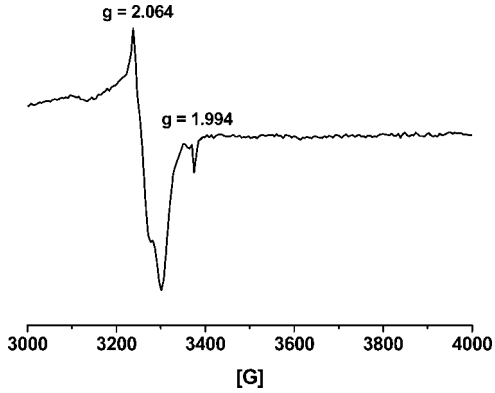

Figure 10. EPR spectrum of $\mathbf{2}^-$ in MeCN at 120 K.

mL) was added to give a brown-black mixture. After the mixture was stirred at –40 °C for 0.5 h, Ph_2PCl (0.05 mL, 0.25 mmol) was added. The new mixture was warmed to room temperature and stirred for 12 h. The same workup as that for the preparation of **2** using acetone/ petroleum ether (v/v = 1:3) as eluent produced **6** as a red solid (0.014 g, 10%), mp 192 °C (dec). Anal. Calcd for $C_{21}H_{18}Fe_2NO_6PS_2$: C, 42.96; H, 3.09; N, 2.39. Found: C, 42.73; H, 3.11; N, 2.36. IR (KBr disk): $\nu_{C\equiv O}$ 2042 (s), 1979 (s), 1960 (vs), 1931 (m) cm^{-1}. ^1H NMR (300 MHz, $CDCl_3$): 2.87 (t, 2H, J = 3.9 Hz, NCH_2CH_2O), 3.81 (d, J = 12.5 Hz, 2H, 2C*H*HS), 3.86 (t, 1H, J = 3.9 Hz, OC*H*H), 3.91 (t, 1H, J = 3.9 Hz, OCH*H*), 3.99 (d, J = 12.5 Hz, 2H, 2CH*H*S), 7.42–7.74 (m, 10H, $2C_6H_5$) ppm. ^{31}P NMR (121 MHz, $CDCl_3$, 85% H_3PO_4): 172.47 (s) ppm. Method ii: A red solution of **D** (0.100 g, 0.23 mmol) in THF (5 mL) was cooled to 0 °C, and then Ph_2PCl (0.05 mL, 0.25 mmol) and Et_3N (0.035 mL, 0.25 mmol) were added. After the new mixture was warmed to room temperature it was stirred overnight. The same workup as that for method i afforded **6** (0.072 g, 53%).

Preparation of [(μ-SCH_2)$_2$N(C_6H_4OMe-*p*)]$Fe_2(CO)_5$[$Ph_2PFe(CO)_2Cp$] (7). To a red solution of **E** (0.043 g, 0.07 mmol) in THF (10 mL) cooled to –40 °C was added *n*-BuLi (1 M in hexane, 0.07 mL). The mixture was stirred at this temperature for 10 min, resulting in a color change from red to brown-black. After $CpFe(CO)_2I$ (0.022 g, 0.07 mmol) was added, the new mixture was warmed to room temparature and stirred for 2 h. The same workup as that for the preparation of **2** gave **7** as a red solid (0.035 g, 60%), mp 210 °C (dec). Anal. Calcd for $C_{33}H_{26}Fe_3NO_8PS_2$: C, 47.92; H, 3.17; N, 1.69. Found: C, 47.72; H, 3.12; N, 1.66. IR (KBr disk): $\nu_{C\equiv O}$ 2039 (s), 2019 (s), 1974 (vs), 1909 (m) cm^{-1}. ^1H NMR (400 MHz, $CDCl_3$): 2.78 (br s, 2H, 2C*H*HS), 3.71 (br s, 5H, 2CH*H*S, OCH_3), 4.77 (s, 5H, C_5H_5), 6.47, 6.48, 6.72, 6.74 (AB quartet, 4H, C_6H_4), 7.35–7.96 (m, 10H, $2C_6H_5$) ppm. ^{31}P NMR (121 MHz, $CDCl_3$, 85% H_3PO_4): 62.79 (s) ppm.

X-ray Structure Determinations of 1, 3, 4, 6, and 7. Single crystals of **1**, **3**, **6**, and **7** suitable for X-ray diffraction analyses were grown by slow evaporation of the CH_2Cl_2/hexane solutions of **1** and **3** at 4 °C, the CH_2Cl_2 solution of **6** at –20 °C, and the THF solution of **7** at –10 °C, respectively, whereas a single crystal of **4** was grown by slow diffusion of MeOH into its CH_2Cl_2 solution at 4 °C. A single crystal of **1**, **6**, or **7** was mounted on a Bruker SMART 1000 diffractometer. Data were collected at room temperature by using a graphite monochromator with Mo Kα radiation (λ = 0.71073 Å) in the $\omega-\varphi$ scanning mode. Absorption correction was performed by the SADABS program.[27] A single crystal of **3** or **4** was mounted on a Rigaku MM-007 (rotating anode) diffractometer equipped with Saturn 70CCD. Data were collected at room temperature, using a confocal monochromator with Mo Kα radiation (λ = 0.71070 Å) in the $\omega-\varphi$ scanning mode. Data collection, reduction, and absorption correction were performed by the CRYSTALCLEAR program.[28] All the structures were solved by direct methods using the SHELXS-97 program[29] and refined by full-matrix least-squares techniques (SHELXL-97)[30] on F^2. Hydrogen atoms were located using the geometric method. Details of crystal data, data collections, and structure refinements are summarized in Tables 3 and 4, respectively.

Electrochemistry and Spectroelectrochemistry (SEC). Acetonitrile (HPLC grade) was used for electrochemistry assays. A solution of 0.1 M *n*-Bu_4NPF_6 in MeCN was used as electrolyte in all cyclic voltammetric experiments. Electrochemical measurements were made using a BAS Epsilon potentiostat. All voltammograms were obtained in a three-electrode cell with a 3 mm diameter glassy carbon working electrode, a platinum counter electrode, and an Ag/Ag^+ (0.01 M $AgNO_3$/0.1 M *n*-Bu_4NPF_6 in MeCN) reference electrode under CO atmosphere. The working electrode was polished with 0.05 μm alumina paste and sonicated in water for 10 min prior to use. Bulk electrolysis was run on a vitreous carbon rod (ca. 3 cm^2) in a gastight H-type electrochemical cell containing 20 mL of MeCN. All potentials are quoted against the ferrocene/ferrocenium (Fc/Fc^+) potential. Gas chromatography was performed with a Shimadzu gas chromatograph GC-9A under isothermal conditions with nitrogen as a carrier gas and a thermal conductivity detector. Bulk electrolysis for IR SEC study was carried out under the same conditions as those described above. During the course of bulk electrolysis a given amount of catholyte was withdrawn at intervals for determining its IR spectrum on a Bruker FT-IR Equinox 55 spectrophotometer.

Acknowledgment. We are grateful to the National Natural Science Foundation of China and the Research Fund for the Doctoral Program of Higher Education of China for financial support.

Supporting Information Available: Full tables of crystal data, atomic coordinates and thermal parameters, and bond lengths and angles for **1**, **3**, **4**, **6**, and **7** as CIF files. This material is available free of charge via the Internet at http://pubs.acs.org.

OM700956E

(27) Sheldrick, G. M. *SADABS*, *A Program for Empirical Absorption Correction of Area Detector Data*; University of Göttingen: Germany, 1996.
(28) *CRYSTALCLEAR 1.3.6*; Rigaku and Rigaku/MSC: The Woodlands, TX, 2005.
(29) Sheldrick, G. M. *SHELXS97*, *A Program for Crystal Structure Solution*; University of Göttingen: Germany, 1997.
(30) Sheldrick, G. M. *SHELXL97*, *A Program for Crystal Structure Refinement* ; University of Göttingen: Germany, 1997.